Mechanical Properties of Simply Supported Prestressed Concrete Beams under Repeated Over-Loadings

By

Hiroshi MUGURUMA*, Megumi TOMINAGA* and Shin OKAMOTO**

(Received June 30, 1966)

Results of an experimental investigation on the mechanical behavior of simply supported prestressed concrete beams under repeated over-loading are described. This load was characterized by higher maximum load near the failure and the relatively slow loading velocity counting at most 100 cycles to the failure. Differences between the dynamic properties of grouted beams and of non-grouted beams under these loadings are also discussed. Test results give many interesting suggestions for the theoretical approach on the load-deformation relation of prestressed concrete baems subject to repeated over-loadings.

It must be noticed that the deformation-dependent change of dissipated energy for the prestressed concrete beam is quite different from that for steel structure and of U-shaped curves.

1. Introduction

Topics of investigation in recent years on the mechanical properties of reinforced and prestressed concrete member have mainly concerned with either strength and deformation of the reinforced and prestressed concrete member under the action of quasi-static monotonically increasing load or fatigue strength of those under relatively small magnitude of load with high frequency. Although the shear failure phenomenon of these members is not well clarified, the final strength theory under the quasi-static monotonically increasing load is already applicable for the actual design purpose with some safety factor. The deformation of the member under the same type of load greatly depends on the bond characteristics between reinforced steel and concrete. However, the recent progress on this subject makes it promising theoretically to predict the deformation of the member. The long history of the research on the fatigue under the highly frequent load gives a number of available results. But, on the other hand, there is such a type of repeated loading as act to the structure during an earthquake and the visit of a typhoon. This loading is

* Department of Architectural Engineering.
** Department of Architecture.

characterized by a higher maximum load near the failure load and the relatively slow loading velocity counting at most 100 cycles to the failure. Following the trend of making the buildings bigger and taller, the influence of this external loading to the structure has been emphasized and the mechanical properties of the concrete under those actions have been noticed as one of the important research subjects.

Some interesting experimental and analytical studies concerning the load-deformation relationship of the reinforced concrete beams under the repeated loading were recently presented[1),2)]. Considering the complete lack of information about the similar behavior of the prestressed concrete member, this report is primarily concentrated on seizing the general aspects of the mechanical properties of the prestressed concrete member under repeated loading with non-reversed amplitude, from which some rational basic assumptions for theoretical analysis continued later may be given. In addition, the experimental technique to carry out such an intermediate type of loading test was investigated.

Creep strains in a short period as well as plastic strain should be considered for the result of the repeated load test with slow loading velocity and overloading level. Although the experimental studies with the model concept by A. M. Freudenthal and others[3)] are available for the non-linear creep of concrete under the high compressive stress during a relatively long period, those creep of concrete accompanying with the ordinary loading in a short period is not clarified. Generally speaking, if the loading is rapid enough, the creep may be almost negligible except the higher loading stage near failure. From the point of view of eliminating such a time dependence, the period of one cycle in the beam test was chosen approximately 2～2.5 minutes.

2. Description of Test

Materials

Concrete used in the test beam consisted of portland cement and natural river sand and river gravel supplied by local commercial dealers in Japan.

The beam specimens in the entire test series were made of Ube portland cement. The mortar test results for the cement in accordance with the specification of Japanese Industrial Standards (mix proportion 1:2, water-cement ratio 65% in weight ratio, curing in 20°C water) gave compressive strengths 122, 225 and 413 kg/cm^2 at the age of 3, 7 and 28 days respectively.

Both of aggregates were produced in the Yasu River of Japan. The sand had a finess modulus of 2.58; the gravel with a nominal size range of 5 to 25 mm had a finess modulus of 6.96. The grading chart of these aggregates is represented in Fig. 1 which may be considered well distributed.

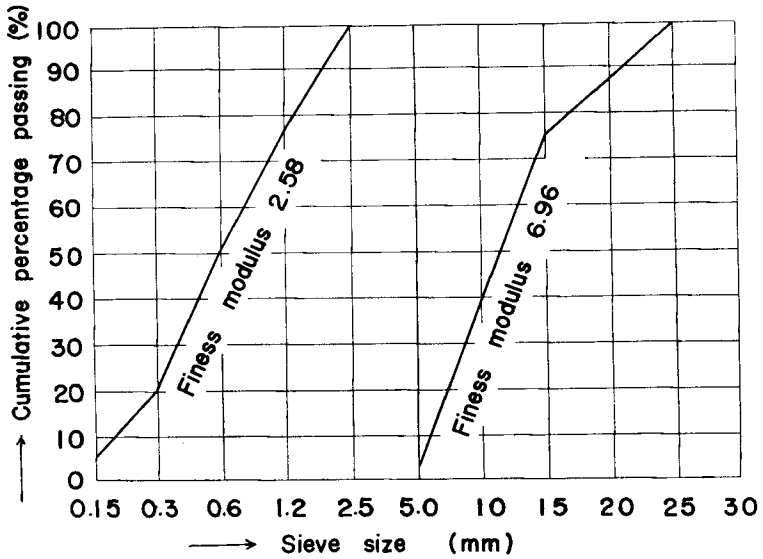

Fig. 1. Grading chart of aggregates.

The concrete mix 1:1.5:3 was used for the entire test series. The mix 1:1.5:3 was intended to represent an intermediate concrete between the solid mass of aggregate and the viscous cement paste, possibly the most popular concrete mix used in prestressed concrete structure. The water-cement ratio of the concrete was 50% which gave a nominal compressive strength of 300 kg/cm^2 at the age of 28 days.

Prestressing tendons used in beam specimens were prestressing steel round bars of nominal diameter 16 mm which were high frequency heat treated and supplied by High Frequency Heat Treatment Co., Tokyo. The allowable stress and the yield stress of the bar were 8940 and 12770 kg/cm^2 respectively. The stress-strain curve of the bar is shown in Fig. 2 including other mechanical quantities.

The anchorage ends of the bar were of nut-anchorplate system at one end and of rivet head burried in concrete at another end. The details of the rivet head end in use are shown in Fig. 3.

Test specimens

Beam dimensions were 12 cm width, 20 cm total depth and 200 cm total length as shown in Fig. 3. The eccentricity of the prestressing bar from the centroid of the beam was 3.5 cm throughout the entire length of the beam. The prestressing bar was inserted into a sheath with a diameter of 22 mm for the purpose of grouting. A couple of small foil strain gages with 15 mm gage length were previously stuck on the tendon in order to measure the steel strain at midspan of the beam during both

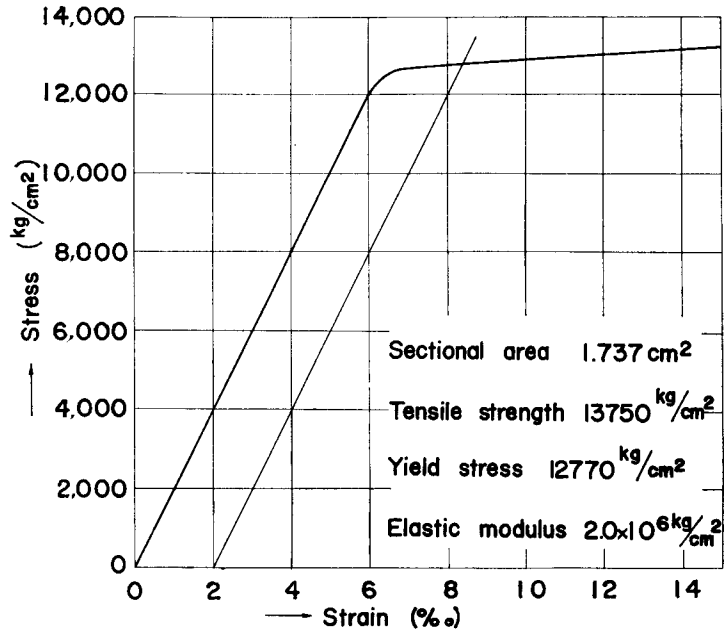

Fig. 2. Mechanical properties of prestressing bar.

prestress transferring operation and repeated loading test. A special protection for these strain gages was prepared. A pair of same beams was cast of fresh concrete of the mechanical properties discussed later. The attached test cylinders of 10× 20 cm were also cast. The beams and the test cylinders were cured at ambient laboratory temperature and humidity in wet burlaps. The prestressing force of 12.5 ton was transferred at approximately 28 days. The amount of the prestress was intended to produce a nominal tensile fibre stress of 2.7 kg/cm² in the extreme edge of compressive concrete and a nominal compressive fibre stress of 107 kg/cm² in the tensile one. The original prestressing force was directly measured by the strain of steel in the beam and indirectly calculated by both the total elongation of the steel at the jacking end and the compressive and tensile extreme fibre strains of concrete. After the prestress transfer, either of the paired beams was grouted with 45% cement paste. The test specimens were left in the laboratory temperature and humidity until the test. The repeated loading tests of the beam were performed at the age of approximately 70 to 80 days. Around the time of the beam test, the repeated loading tests of the attached test cylinders were also performed. The effective prestresses were calculated from the compressive and tensile extreme fiber strains of concrete at the midspan of the beam. A contact type strain gage was used for these measurings.

Loading setup

Experimental setup is shown in Fig. 3. The test beams were placed on the supports fixed on the rigid prestressed concrete testing bed. These supports were composed of both the roller between two parallel smooth steel plates at one end of the support and the spherical steel ball bearing at another end. It was found from the authors' experimental experience that an efficient support mechanism of a simply supported beam should be devised, especially under the repeated over-loading because of the large deformation of the test beam.

The sine-waved repeated force, produced by a 10ton Amsler type pulsator and guided into a dynamic jack which was vertically hanged from the reaction steel frame fixed to the prestressed concrete bed, was applied at the third points of the 180 cm span of test beam through a load-distribution steel I-beam under which the roller-spherical ball loading mechanisms were also prepared.

Measuring instruments

The layout and the block diagram of measuring instruments are shown in Fig. 3 and 4 respectively. Since the loading was performed with relatively rapid velocity and a large number of deformation readings should be recorded simultaneously, electronical automatic measuring and recording systems were extensively used in the experiments. For the purpose of measuring the magnitude of the load, a load cell using wire strain gages was inserted between the jack and the load-distributing steel I-beam as shown in Fig. 3. The magnitude of the midspan deflection of the test beam was converted into the displacement of the core of a differential transformer with a non-stretching and flexible nylon string through pulleys.

A X-Y pen recorder with electronically automatic balancing potensiometers was used for the recording of load-deflection curves. The monitor to the mechanical stage of the test beam during experiments was easily made by watching the curves on X-Y pen recorder. The compressive and tensile extreme fiber strains of concrete were measured with both wire strain gages bonded directly on it and differential transformers fixed to a pair of rectangular aluminium yokes apart by 400 mm at midspan of the beam. The strain of the prestressing bar during the test was measured by foil gages prepared at the time of casting. All of the informations regarding these strain data as well as the magnitude of load were recorded by a electro-magnetic oscillograph of direct visual multi-channel type.

Both of the X-Y recorder and the oscillograph had enough responce speeds to sweep the full scale of range, comparing with the velocity of load application and deformation occurrence. The sinking of the rivet head of the prestressing bar was checked by a 1/1000 mm dial gage.

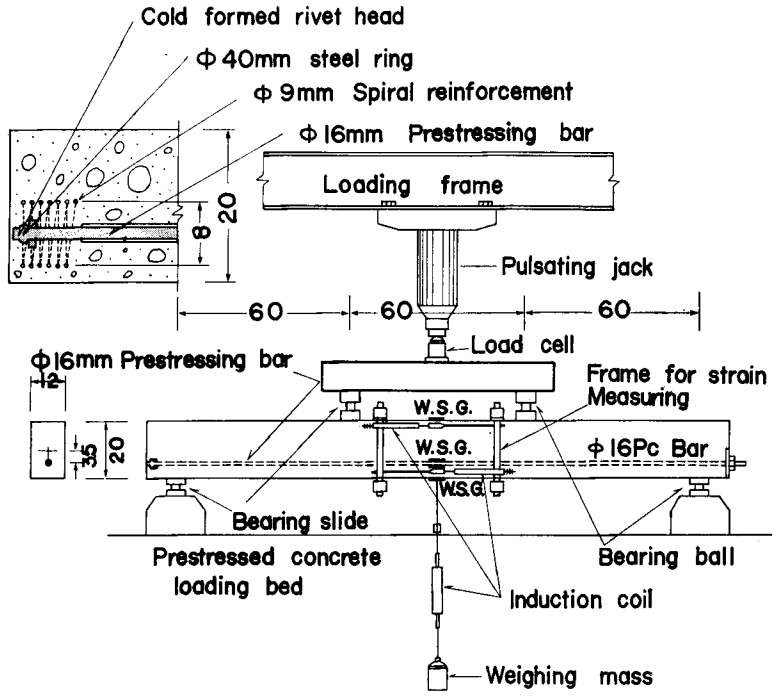

Fig. 3. Loading and measuring setup (Unit: cm).

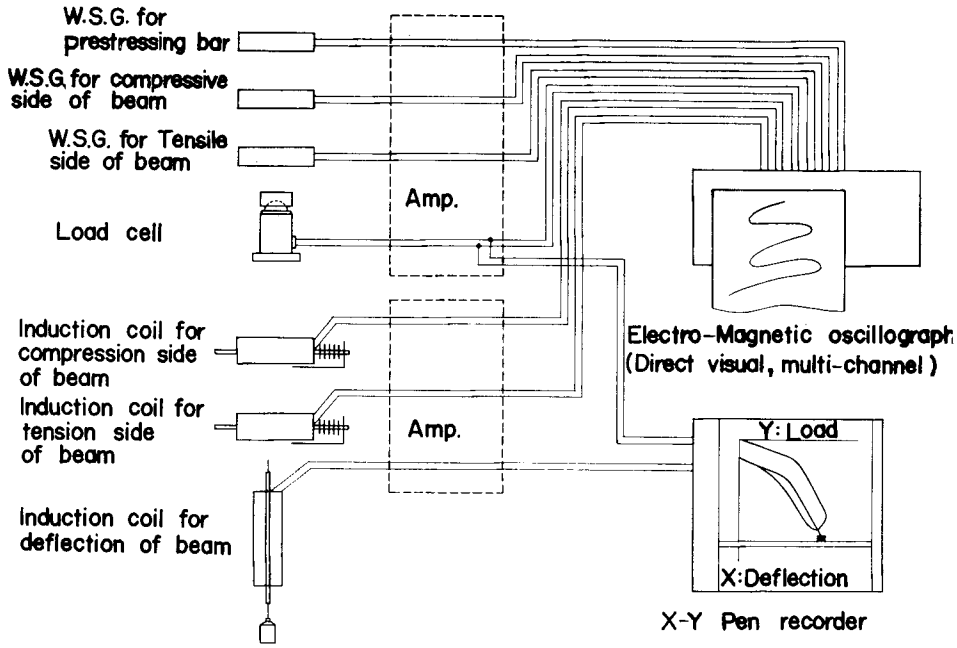

Fig. 4. Block diagram of measuring method.

Table 1. Test Results

Test Specimen	Effective prestressing force in ton	Calcutated eccentricity in cm	Age of test in days	Concrete strength in kg/cm²		Cracking load in ton		Failure load in ton		Loading		Max. comp. fiber strain for initial loading	Number of loading cycles before failure occurred
				Comp.	Tens.	Obser.*1	Calcu.*2	Obser.	P/P_u*3				
PG-1	10.88	3.50	70	352	36.1	3.75	4.32	8.65	0.90	Repeatedly increasing	Static	—	—
PN-1	11.57	3.61	73			4.00	4.54	7.15	0.87				
PG-2	8.69	3.52	70	336	33.2	4.55	3.97	9.75	1.00	Monotoneously increasing			
PN-2	10.09	3.34	70			4.50	4.06	8.20	1.00				
PG-3	10.94	3.17	80	428	35.4	4.01	4.31	—	—	Repeated (Max. strain -constant)			
PN-3	10.63	3.27	72			4.00	4.32	—	—				
PG-4	10.17	3.41	76	343	35.9	3.90	4.27	6.80	0.70	Repeated (Max. load -constant)	1～50 S.*4 51～1000 D.*5	1.30‰	(1,000)*7
PN-4	10.12	3.08	79			4.20	3.97	6.10	0.71		1～10 S. 11～1000 D.	1.51‰	(1,000)*7
PG-5	10.71	3.37	74	308	35.7	4.56	4.20	7.85	0.81		1～50 S. 51～395 D.	2.10‰	395
PN-5	12.05	3.27	76			4.00	4.17	—	—		1～26 S. 27～1000 D.		(1,000)*7
PG-6	—	3.37	83	396	41.0	4.90	—	7.85	0.81		1～10 S. 11～120 D.	(2.25‰)*6	120
PN-6	10.58	3.68	79			3.80	4.30	6.45	0.76		1～12 S. 13～227 D.	(2.25‰)	22
PG-7	9.88	3.23	82	390	37.2	4.10	4.02	8.45	0.87		1～18 S.	(2.50‰)	18
PN-7	10.58	3.37	78			4.10	4.42	6.90	0.81		1～10 S. 11～1000 D.	(2.50‰)	(1,000)*7
PG-8	9.70	3.40	85	336	32.8	4.15	3.93	8.65	0.89		1 S.	(3.00‰)	1
PN-8	9.80	3.34	82			3.80	3.92	7.25	0.85		1 S.	(3.00‰)	1
PG-9	10.10	3.33	86	—	38.4	4.55	4.15	8.80	0.91		1～9 S.	2.73‰	9
PN-9	11.10	3.33	87			4.32	4.37	7.18	0.84		1～21 S.	2.82‰	21
PG-10	—	3.37	81	344	36.0	—	—	—	—		S.		
PN-10	—	3.37	84			4.22	—	7.08	0.83		1～13 S.	2.94‰	13

*1 Observed value, *2 Calculated value, *3 Ratio of repeated failure load to non-repeated, *4 Static, *5 Dynamic,
*6 Presumed value (miss operation of recording apparatus), *7 Did not fail by 1,000 cycles.

Test procedure

A pair of grouted and non-grouted beams cast at the same time were tested under the same loading conditions. The tests of beams were carried out at the age of approximately 70 to 85 days. The kinds of loading types were classified into three groups; monotonically increasing load, repeated loading with constant compressive fiber strain of concrete and repeated loading with constant maximum load depending on the various magnitude of the initial compressive fiber strain of concrete. The setting of the initial compressive fiber strain ranged from 1.3‰ to 3.0‰. The period necessary for one cycle of the repeated loading was about 2.5 min. regardless of the maximum load level. If the beam was not crushed when the relation between its load and deformation under repeated load reached almost steady state, the loading period was shortened to 2 sec. The repeated test on the attached test cylinders was performed with the constant stress rate of 2 kg/cm²/sec.

3. Test Results

Load-deformation relation

Typical load-deflection curves are shown in Fig. 5 to 7. Fig. 5 shows the relation between load and deflection at the midspan of the beam PG-5 which endured a relatively large number of load cycles. Fig. 6 and 7 show a comparison between grouted beam PG-9 and non-grouted one PN-9 which failed at the 10th and 22nd loading cycles respectively. Fig. 8 and 9 show typical relations between extreme fiber strain of concrete and applied load. Some of these strain data were

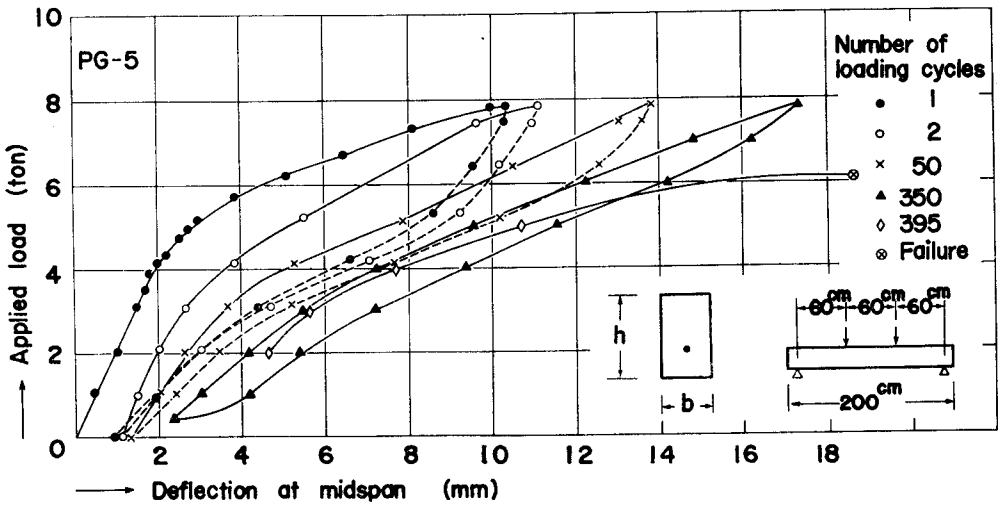

Fig. 5. Typical load-deflection curves of grouted beam.

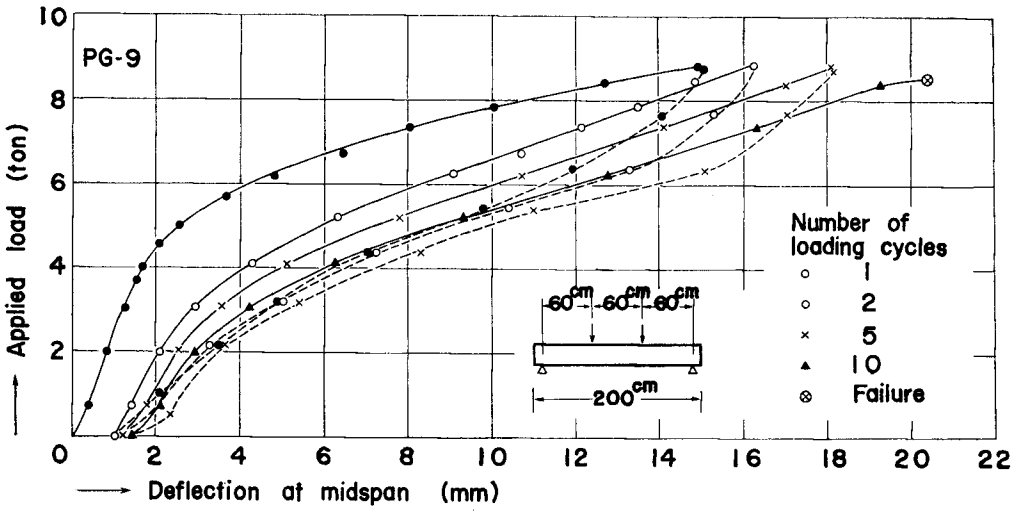

Fig. 6. Typical load-deflection curves of grouted beam.

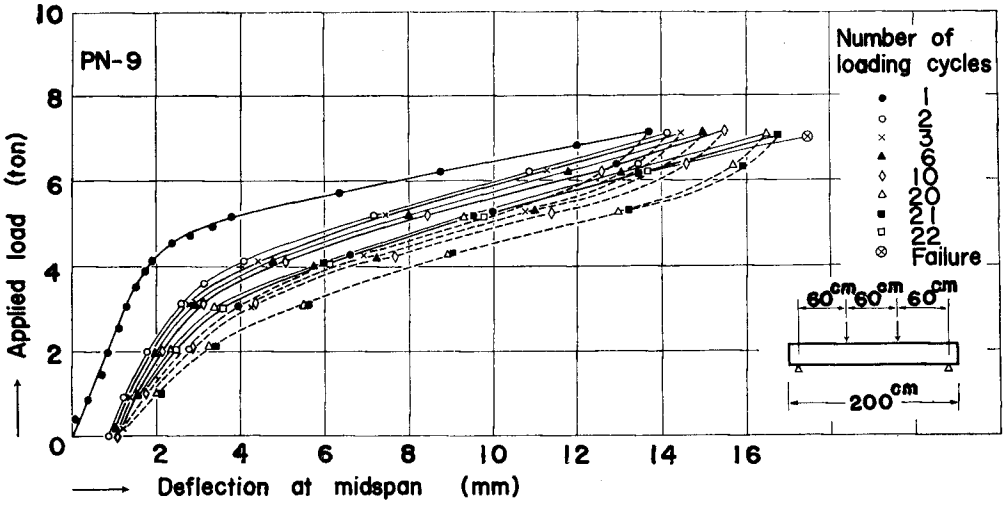

Fig. 7. Typical load-deflection curves of non-grouted beam.

missed because a few of the cracks of concrete were occurred outside of the gage length of the measuring instruments. The number of tensile cracks of concrete due to bending were at most three. Therefore, the gage length always inclined to miss the mean extreme fiber strains of concrete.

While the loading cycles were increased, the compressive extreme fiber strain of concrete was also increased from the initially set value. A diagrammatic representation of this behavior is Fig. 10, omitting some of the obtained data due to

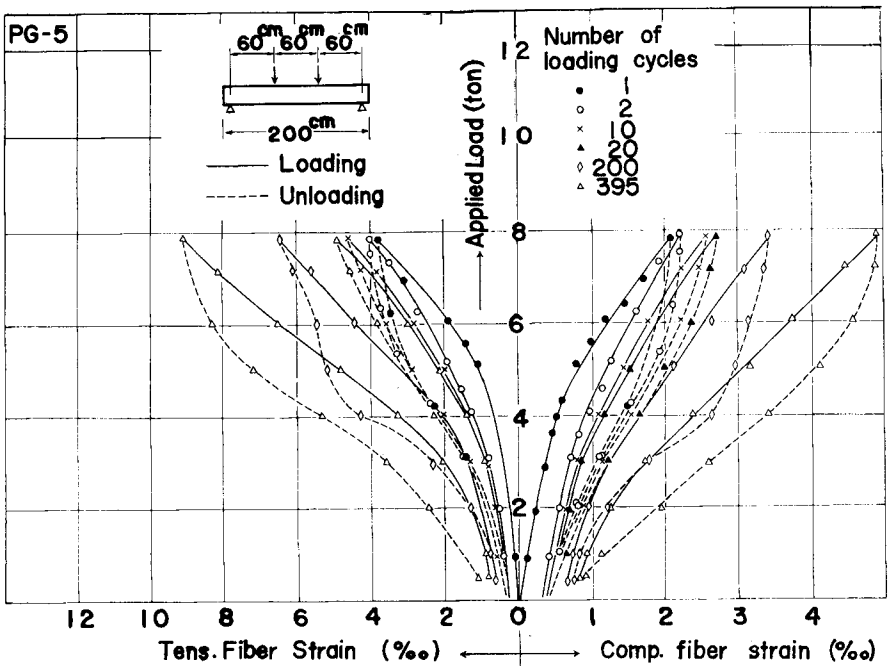

Fig. 8. Relation between extreme fiber strain and applied load for PG-5 beam.

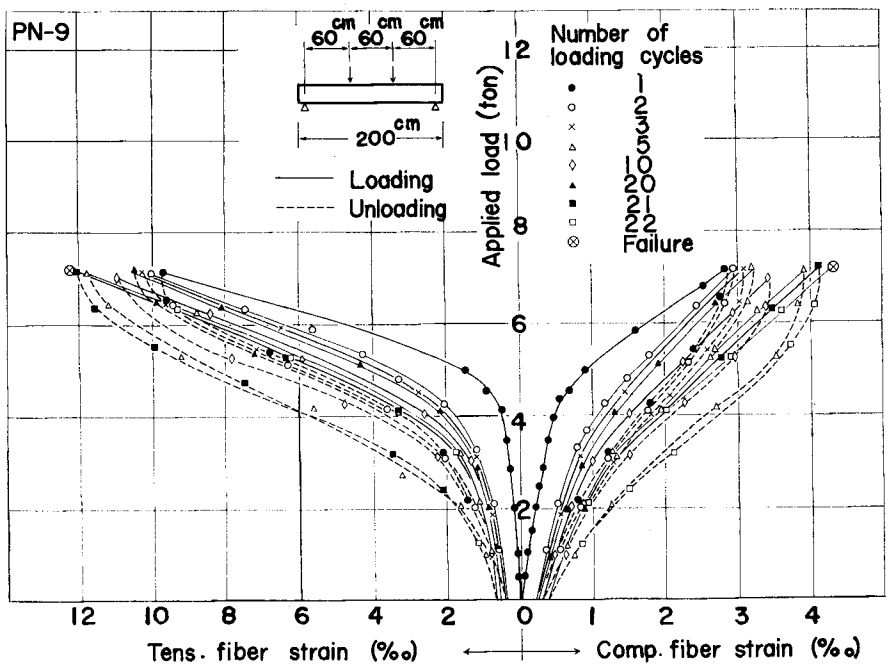

Fig. 9. Relation between extreme fiber strain and applied load for PN-9 beam.

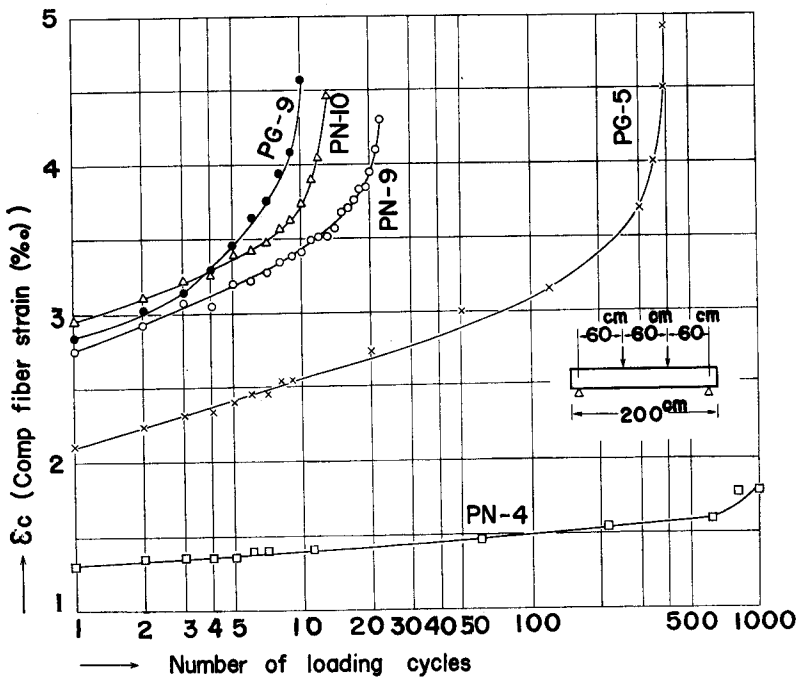

Fig. 10. Relation between comp. fiber strain and number of loading cycles.

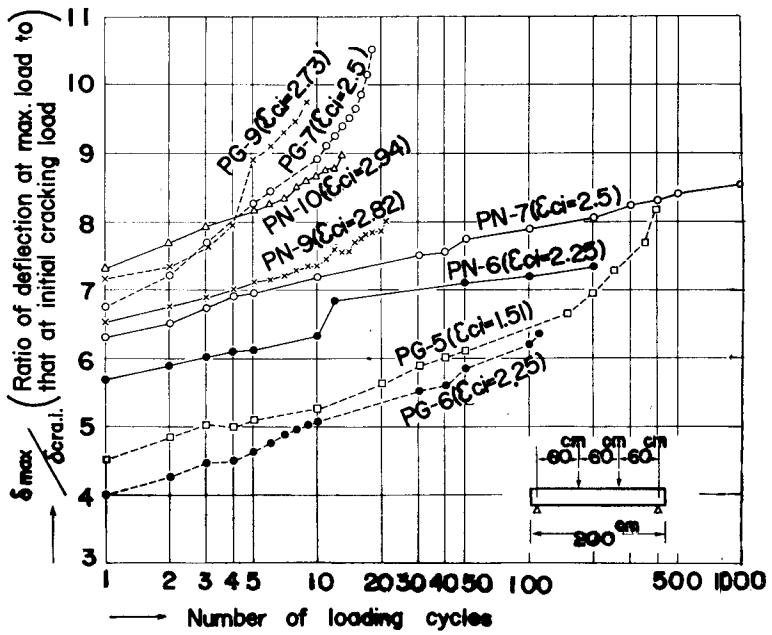

Fig. 11. Relation between $\delta_{max.}/\delta_{cra.i.}$ and number of loading cycles.

above described reason. Fig. 11 shows the relation between the ratio of deflection $\delta_{max.}$ at the maximum load to that $\delta_{cra.i.}$ at the initial cracking load and the number of loading cycles. Rate of increase in $\delta_{max.}/\delta_{cra.i.}$ is higher in grouted beams than in non-grouted ones because of the gradual loss of bond. Fig. 10, 11 and 12 show the relation between the ratio of the cracking load $P_{cra.}$ in each subsequent loading cycle to that $P_{cra.i.}$ in the initial cracking load and the number of loading cycles. The decrease of the ratio $P_{cra.}/P_{cra.i.}$ is noteworthy in the first reloading stage but is inclined to be smaller in subsequent reloading. For the nongrouted beam the decrease of the ratio $P_{cra.}/P_{cra.i.}$ is inversely proportional to the magnitudes of the initially set compressive extreme fiber strain of concrete and for the grouted beam is proportional to those.

Rigidity

Fig. 13 and 14 show the relation between applied moment and bending stiffness. From the graphs, it may be conjectured that the differences of the rigidity at initial loading and at subsequent reloading were remarkable, and the rigidity at unloading was very rapidly decreased for the non-grouted test beam while it was gradually decreased for the grouted one.

Fig. 15 shows the change of the ratio K_i^*/K_i, where K_i is the initial bending stiffness in first loading and K_i^* is that in each subsequent reloading, against the number of loading cycles. It seems that the bond in the grouted beam is fairly effective to hold the initial bending stiffness. The action of over-load seems to result in a remarkable decrease of K_i^*/K_i.

Failing load

The ratio of the magnitude of repeated failing load P to that of the failing load Pv under the monotonically increasing load was plotted against the maximum compressive extreme fiber strain ε_{ci} of concrete for the initial loading as shown in Fig. 16. This shows the greater differences of P/Pv between the grouted beam and the non-grouted one at higher strains ε_{ci}. Fig. 17 shows the endurance number of loading for the beam with various ε_{ci}. Comparing with the corresponding non-grouted beam, the failure of the grouted beam occurs earlier, because the miximum constant load for the grouted beam exceeds the equivalent magnitude of load for the non-grouted one due to the rapid loss of bond.

Sinking of rivet head

Fig. 18 represents the sinking of the rivet head of the prestressing bar. The grouted and non-grouted beams with large value of ε_{ci} produce a large amount of rapidly increasing sinking, though the initial sinking of the rivet head for the grouted beam is relatively small.

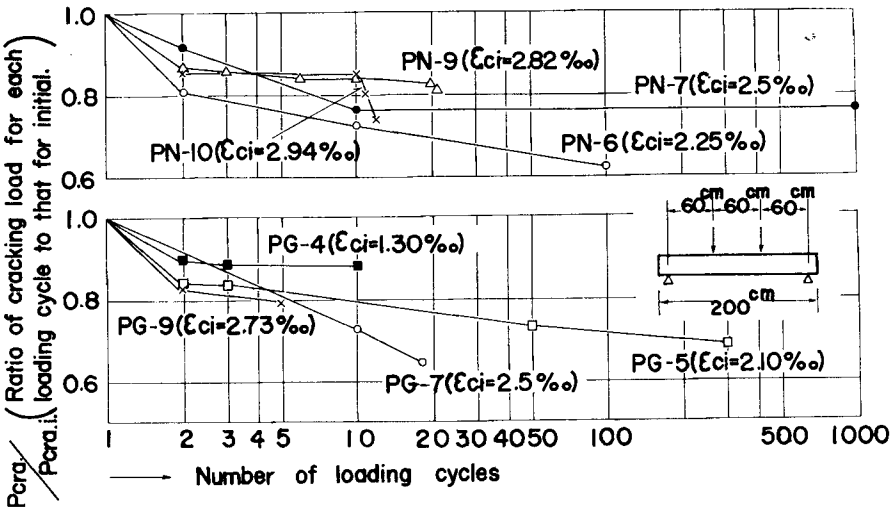

Fig. 12. Relatiot between $P_{cra.}/P_{cra.i.}$ and number of laoding cycles.

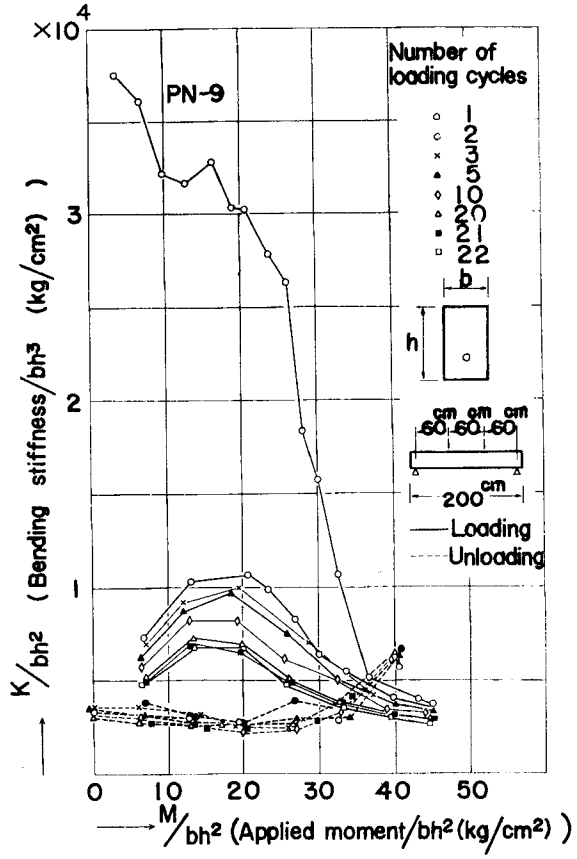

Fig. 13. Relation between K/bh^3 and M/bh^2 for PN-9 beam.

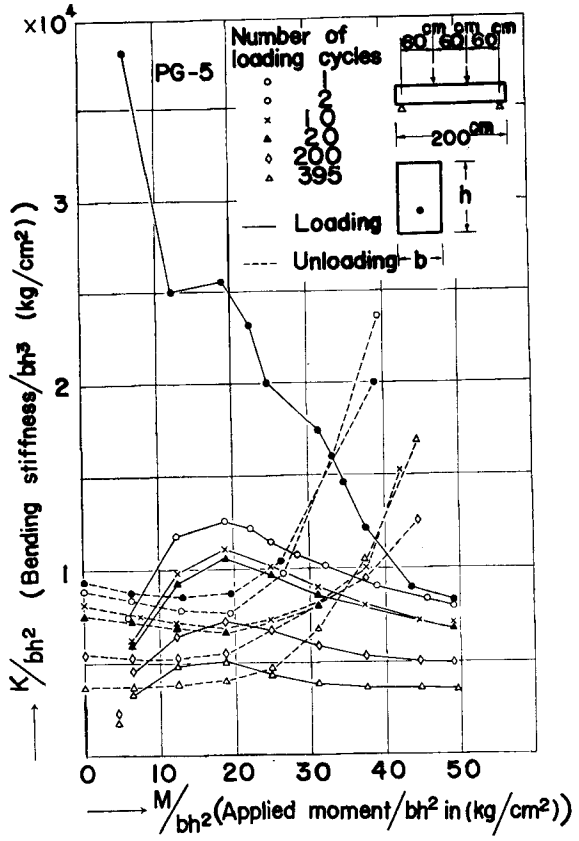

Fig. 14. Relation between K/bh^3 and M/bh^2 for PG-5 beam.

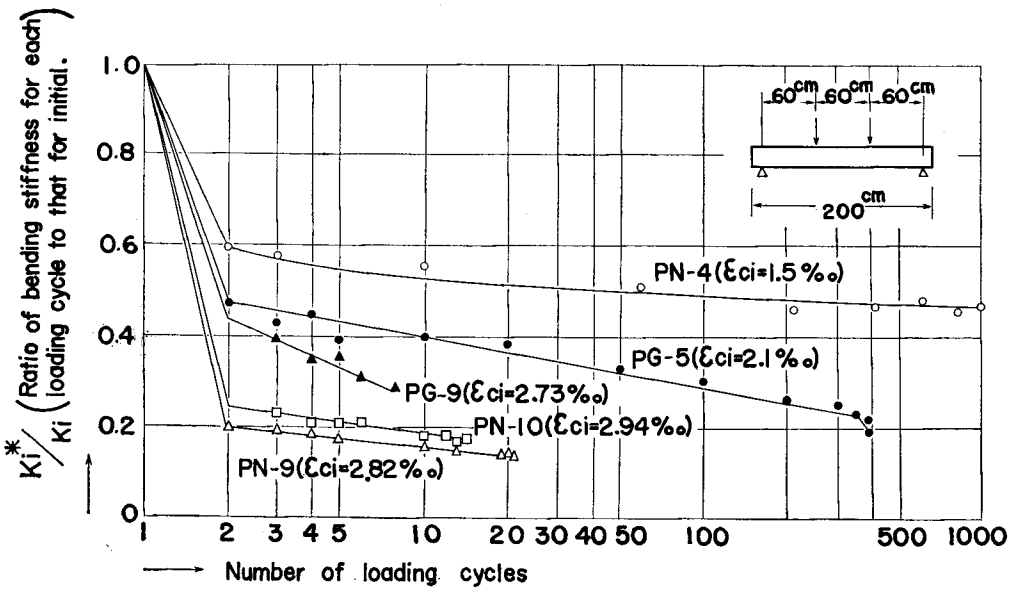

Fig. 15. Relation between K_i^*/K_i and number of loading cycles.

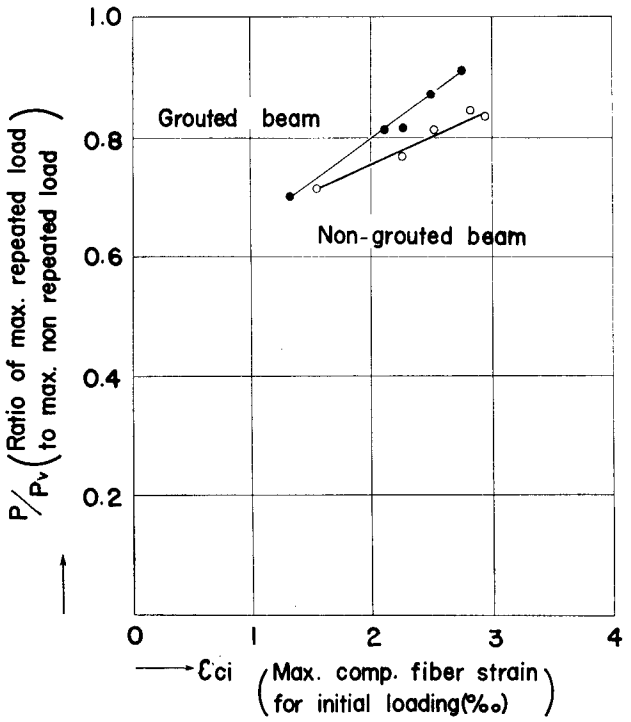

Fig. 16. Relation between P/P_v and max. compressive fiber strain.

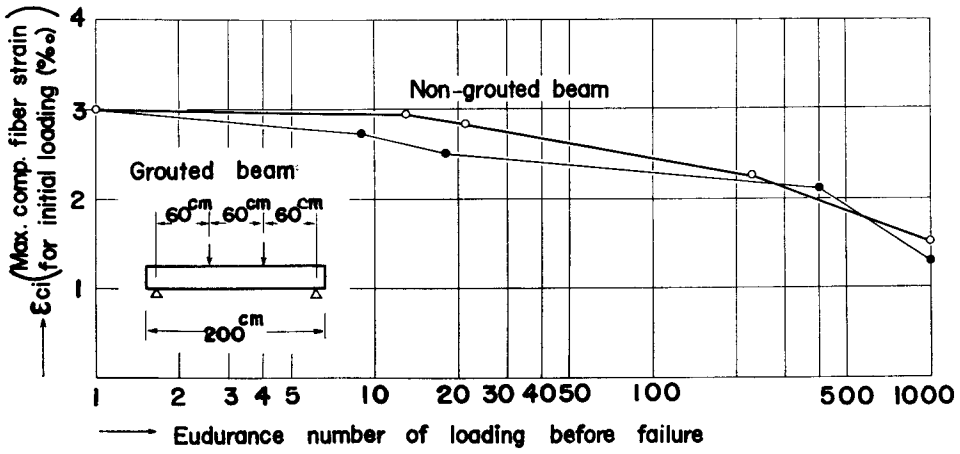

Fig. 17. Relation between max. comp. strain for initial loading and number of loading cycle before failure occurred.

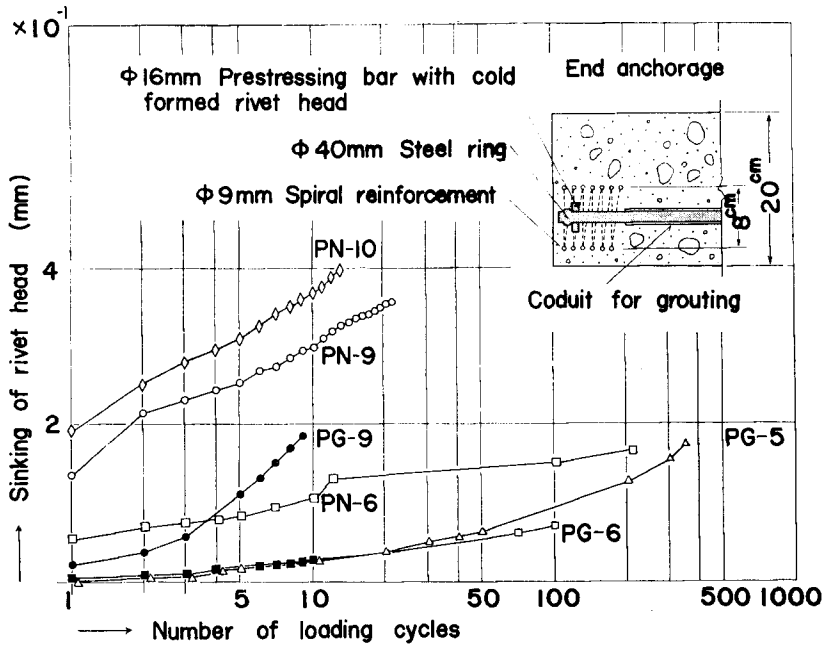

Fig. 18. Relation between sinking of rivet head and number of loading cycles.

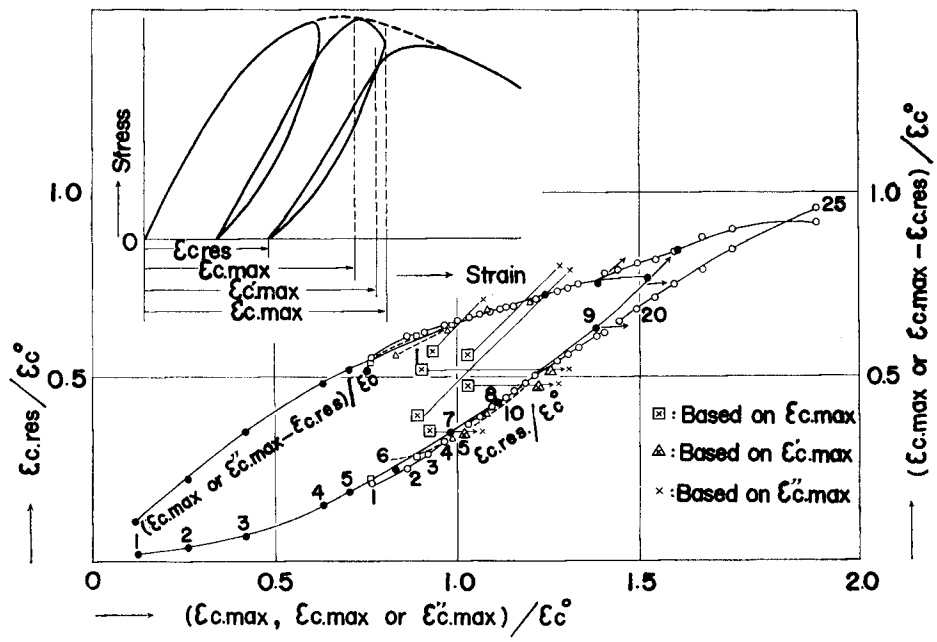

Fig. 19. Property of stress-strain curve of concrete.

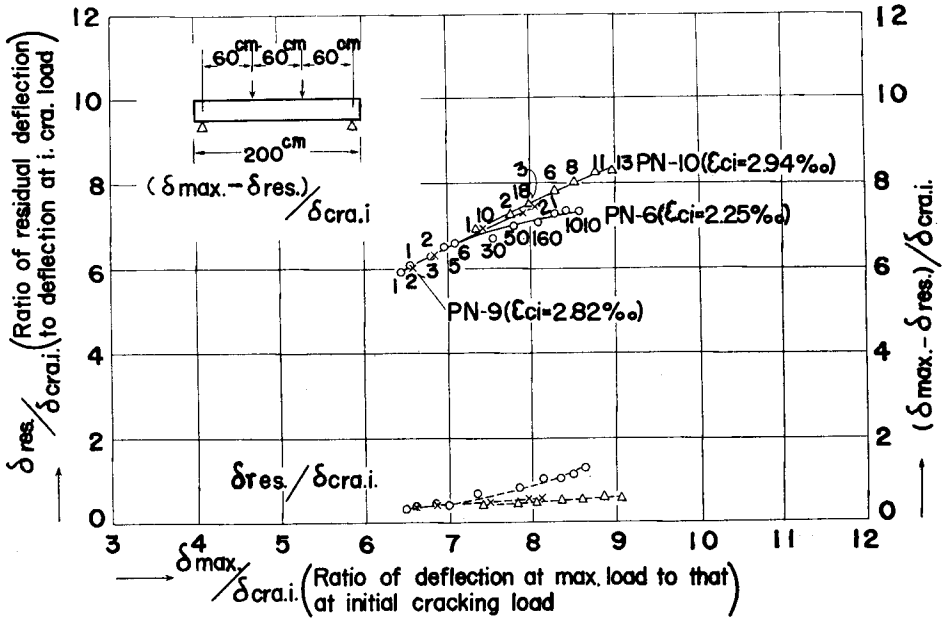

Fig. 20. Property of load-deflection curves for non-grouted beams.

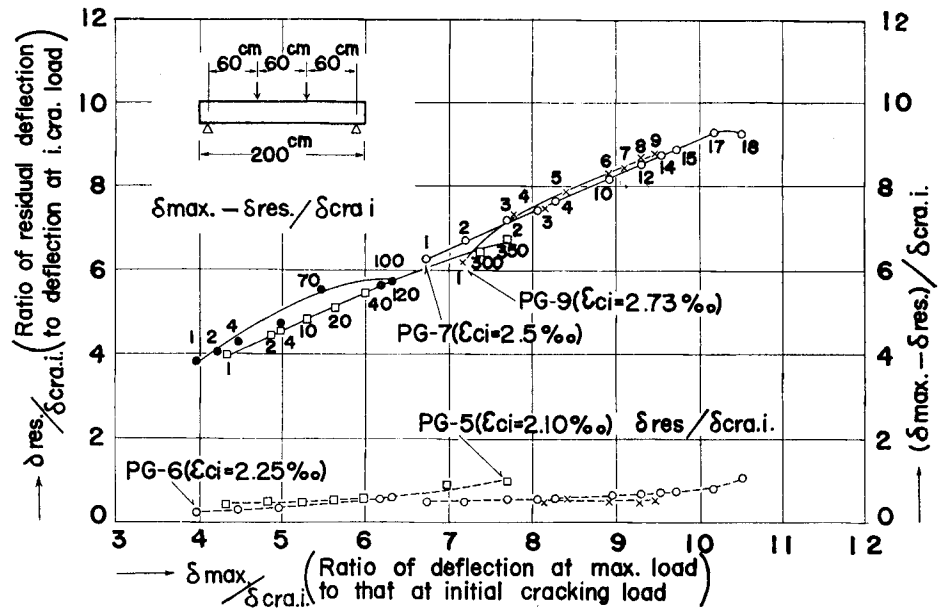

Fig. 21. Property of load-deflection curves for grouted beams.

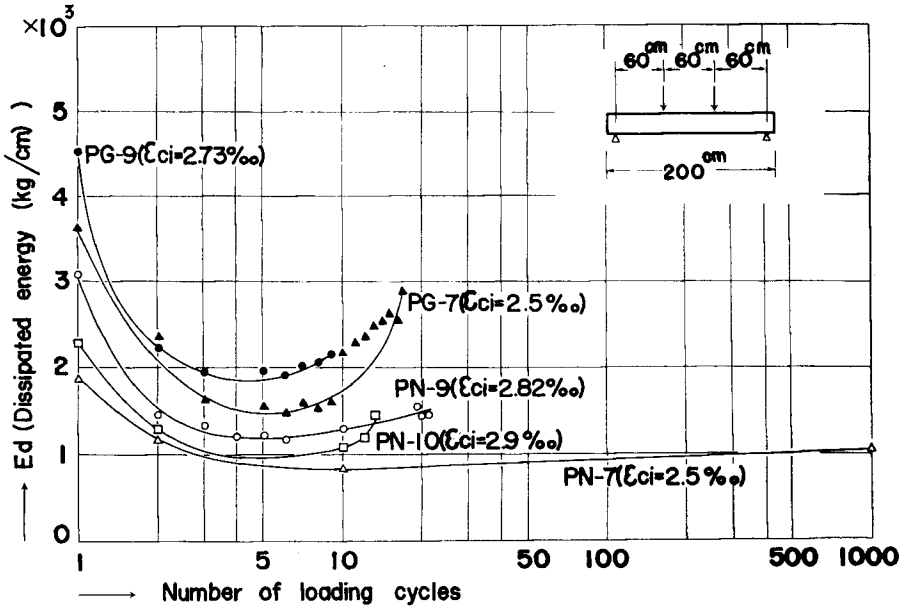

Fig. 22. Relation between dissipated energy and number of loading cycles.

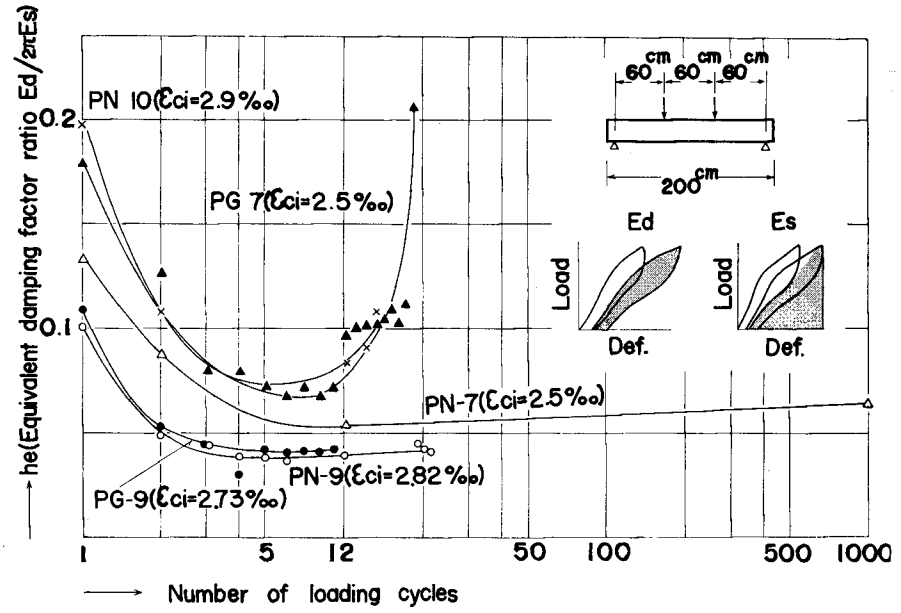

Fig. 23. Relation between equivalent damping factor ratio and number of loading cycles.

Uniqueness of load-deflection curves

Fig. 19 shows a result of repeated loading test for the 10×20 cm test cylinder. The values of the residual strain $\varepsilon_{c.res.}$ and the elastic strain $\varepsilon_{c.max.}-\varepsilon_{c.res.}$ are plotted against the strain $\varepsilon_{c.max.}$ at maximum stress by dividing the original value with the value of the strain ε_c^0 at maximum stress of the mean stress-strain curve obtained by monotonically increasing loading. Almost all of these points are located on the single lines. Taking the strain $\varepsilon'_{c.max.}$ or $\varepsilon''_{c.max.}$ instead of $\varepsilon_{c.max.}$, the ill-situated points are also coincided with the lines. This means that the uniqueness of stress-strain relation is likely to be true except the higher stress stage.

For the load-deflection curves, similar charts are made. Fig. 20 and 21 show those charts for non-grouted and grouted beams respectively. Glancing over these charts the uniqueness of load-deflection curves is also likely to be true.

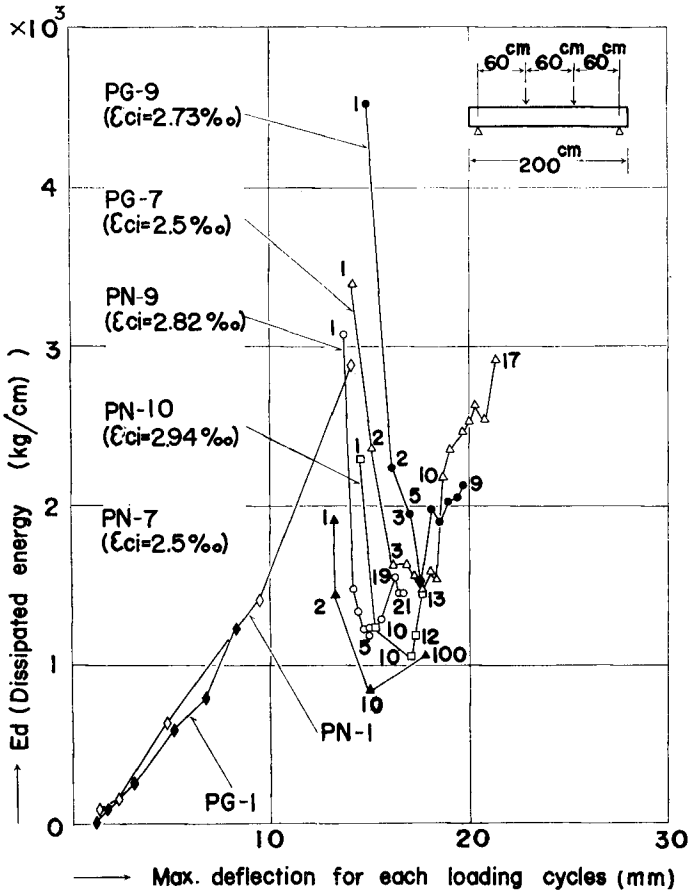

Fig. 24. Relation between dissipated energy and max. deflection for each loading cycle.

Dissipated energy

Although the dissipated energy per unit segment of the beam subject to bending should be computed on the moment-curvature charts, Fig. 22 and 23 are based on load deflection curves.

Fig. 22 shows the change of dissipated energy E_d during each of the loading cycles plotted against the number of loading cycles. Fig. 23 shows the change of the equivalent damping factor ratio *he*. The dissipated energy E_d for the grouted beam is larger than that for the non-grouted beam because of the higher constant maximum load. The change of E_d and *he* is characterized by U-shaped curves. Fig. 24 shwos the change of dissipated energy E_d plotted against the maximum deflection of each loading cycle. Minimizing the small difference among test specimens, a graph with dimensionless quantities instead of Fig. 24 is obtained in Fig. 25. It is found that the change of dissipated energy for the prestressed concrete

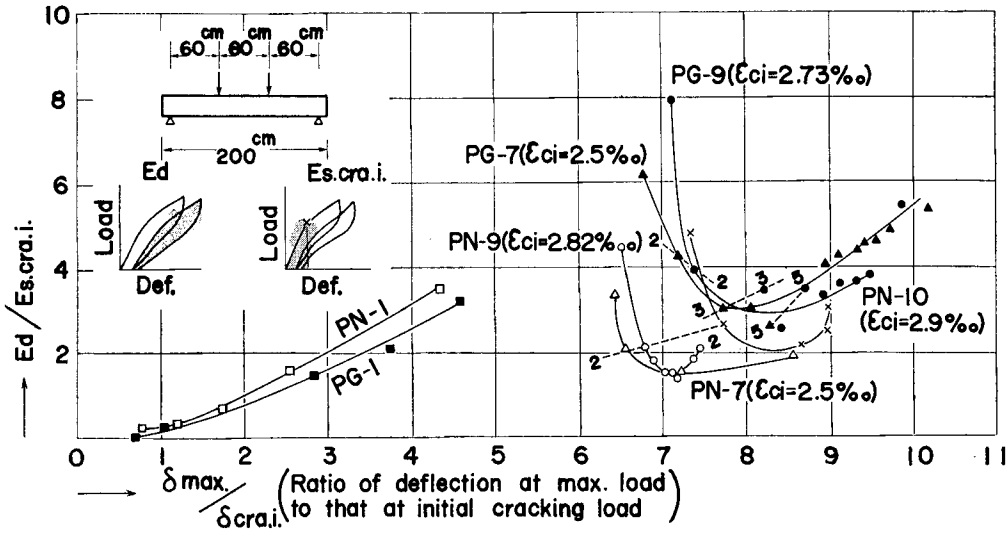

Fig. 25. Relation between $E_d/E_{d.cra.i.}$ and $\delta_{max.}/\delta_{crai.i.}$

beam is quite different from that for steel structure and of U-shapec curves. Also, it is found that the dimensionless quantities $E_d/E_{s.cra.i}$ for grouted beams show larger value than those for non-grouted beams. The somewhat distinguished tendency and clear grouping of the $E_d/E_{s.cra.i.}$ curves between the grouted beam and the non-grouted one may be understood as a suggestion for uniqueness of each load-deflection curve.

4. Conclusive Remarks

The experiment reveals the following facts on the behavior of the simply

supported prestressed concrete beams under the repeated over-load.

1. Excepting the range of higher load level causing the possible incremental deformation, the load-deformation curve of the test beam under cyclic load seems to have a unique vector regardless of the preceding load history. Although the noteworthy difference of the deformation between grouted and non-grouted beam exists in first or some subsequent loading cycles, it becomes smaller afterwards. This is caused by rapid loss of bond.

2. The application of repeated constant maximum load, causing more than the compressive initial extreme fiber strain ε_{ci} of about 2.3‰ in the concrete of the grouted beam and about 2.5‰ in the concrete of the non-grouted one, results in failure due to crushing of compressive concrete by 100 cycles.

3. Under the loading condition to repeat the constant maximum load leading to such a failure, the fall of failing loading under repeated load from that under monotonically increasing load is about 20% for both of grouted and non-grouted beams. It is remarkable that under such a repeated loading the grouted beams show lower capacity of load than the non-grouted one.

4. The curve of the dimensionless dissipated energy $E_d/E_{s.cra.i}$ against the dimensionless maximum deflection $\delta_{max.}/\delta_{cra.i.}$ is characterized by the U-shapes which decrease with steep inclination in the smaller $\delta_{max.}/\delta_{cra.i.}$, then reach the bottoms at the value of 7 to 8 in $\delta_{max.}/\delta_{cra.i.}$ and afterwards increase with relatively mild inclination. Higher values of ε_{ci} tend to produce narrow U-shapes with the rapid change of the curvature.

Notaion

E_d : Dissipated energy in each loading cycle
E_s : Equivalent viscous dissipated energy in each loading cycle
$E_{s.cra.i.}$: Stored energy at initial cracking load
he : Equivalent damping factor ratio
K : Bending stiffness
K_i : Initial bending stiffness for first loading
K_i^* : Initial bending stiffness for reloading
P_v : Failure load for monotonically increasing load
P : Constant maximum load for repeated loading
$P_{cra.i.}$: Initial cracking load
$P_{cra.}$: Cracking load for subsequent reloading
ε_c : Compressive extreme fiber strain of concrete
ε_{ci} : Maximum strain initially set at the compressive extreme fiber of concrete

$\varepsilon_{c.max.}$: Compressive strain at maximum stress in stress-strain curves of concrete obtained by cylinder test

$\varepsilon'_{c.max.}$: Compressive strain at the point on reloading curve intersecting the immediately preceding unloading curve in stress-strain curves of concrete obtained by cylinder test

$\varepsilon''_{c.max.}$: Maximum strain at each loading cycle in stress-strain curves of concrete obtained by cylinder test

$\varepsilon_{c.res.}$: Instantaneous residual strain at each loading cycle in stress-strain curves of concrete obtained by cylinder test

ε_c^0 : Compresive strain at the maximum stress in mean stress-strain curves of concrete obtained by cylinder test under monotonically increasing load

$\delta_{res.}$: Instantaneous residual deflection at the midspan of beam in each loading cycle

$\delta_{max.}$: Maximum deflection at the midspan of beam in each loading cycle

$\delta_{cra.i.}$: Deflection at the midspan of beam at initial cracking load

References

1) B.P. Sinha, K.H. Gerstle and L.G. Tulin; Response of Singly Reinforced Beams to Cyclic Loading, J. Amer. Concr. Inst., Proceedings V. 61, No. 8, pp. 1021, 1038 (1964).

2) G.L. Agrawal, L.G. Tulin and K.H. Gerstle; Response of Doubly Reinforced Concrete Beams to Cyclic Loading, J. Amer. Concr. Inst., Proceedings V. 62, No. 7, pp. 823, 835 (1965).

3) A.M. Freudenthal and F. Roll; Creep and Creep-Recovery of Concrete under High Compressive Stress, J. Amer. Concr. Inst., Proceedings V. 54, pp. 111, 1142 (1958).